Development of reduced and optimized reaction mechanisms based on genetic algorithms and element flux analysis

Federico Perini[a,*], Jessica L. Brakora[b], Rolf D. Reitz[b], Giuseppe Cantore[a]

[a]*Dipartimento di Ingegneria Meccanica e Civile, Università di Modena e Reggio Emilia, Modena, Italy*
[b]*Engine Research Center, University of Wisconsin–Madison, Madison, 53706, USA*

Abstract

The present paper introduces an approach for the automatic development of reduced reaction mechanisms for hydrocarbon combustion. An iterative reduction procedure is adopted with the aim of gradually reducing the number of species involved in the mechanism, while still maintaining its predictiveness in terms of not only ignition delay times, but also the time evolution of important species. In particular, a global error function is defined taking into account a set of 18 ignition delay calculations at different, engine-relevant, initial mixture compositions, temperatures and pressures. The choice of the species to be deleted is performed exploiting the element flux analysis method, first introduced by Revel et al.; when a global error function of the reduced mechanism exceeds the required accuracy, the collision frequencies and activation energies of selected reactions are corrected by means of a GA-based code. The procedure is repeated until the lowest number of species at the required global error tolerance is achieved. The methodology is applied to a detailed mechanism of ethanol combustion consisting of 58 species and 383 reactions to produce an optimal reduced mechanism of 33 species and 155 reactions.

Keywords: mechanism reduction, genetic algorithms, reduced mechanism, element flux, ethanol

*Corresponding author. Tel.: +39 059 2056101; Fax: +39 059 2056126.
Email address: `federico.perini@unimore.it` (Federico Perini)

1. Introduction

The need for complete understanding of the physics and chemistry of combustion phenomena, together with constant progress in computer technology, is currently driving research into adopting full or detailed reaction mechanisms in CFD computations [1, 2]. A wide variety of mechanisms has been developed in recent years for hydrocarbon fuels consisting of tens to hundreds of species and hundreds to thousands of reactions [3–11]. However, mechanism reduction is still mandatory for most practical computations, and research is very active in identifying techniques for obtaining accurate estimates of reaction kinetics with limited computational needs. For example, research for new combustion concepts for internal combustion engines (such as HCCI, homogeneous-charge compression ignition and RCCI, reactivity-controlled compression ignition) has been made possible in recent years by the adoption of CFD codes which are capable of computing complete reaction mechanisms [12, 13], as current pollutant regulations are leading to an increasing need for accurate predictions of the spatial distribution and time evolution of species within the combustion chamber. However, the adoption of full or detailed reaction mechanisms in multi-dimensional studies is still too computationally demanding, and the development of accurate reduced mechanisms is of fundamental importance for maintaining the predictive capabilities of the simulations.

1.1. Literature review

A number of techniques have been developed for analyzing detailed combustion mechanisms, and then identifying sets of species and reactions which may be unimportant at certain reacting conditions. These methodologies have been exploited for both the generation of skeletal, reduced mechanisms [14–19], and for accelerating the computation of chemical kinetics during CFD simulations [20–23]. A first class of methods involves the selection of a subset of species and reactions from the detailed mechanism. Among them are sensitivity analysis [24, 25], Directed Relation Graph (DRG) [26], even with error propagation control (DRGEP) [27], principal component analysis (PCA) [28, 29], element flux analysis (EF) [16, 21, 30], single- and multi-objective optimization [15, 17, 18, 31–36]. A second category involves instead techniques aiming at identifying and separating the different timescales acting at the same time. This allows one to solve part of the reacting system in terms of algebraic equations, or eventually to reduce its stiffness. Besides

the classical quasi steady-state (QSS) and partial equilibrium approximations (PE) [37–39], and computational singular perturbation (CSP) [40, 41], which, allowing fast and slow time scales analysis, has extensively been used also for generation of reduced and skeletal mechanisms [42–45], other methodologies have been recently developed, such as intrinsic, trajectory-generated, constraint-defined low-dimensional manifolds (ILDM, TGLDM, CDLDM) [46–48], rate-controlled constrained equilibrium (RCCE) [49, 50], invariant manifold methods (MIM) [51], and invariant constrained equilibrium edge preimage curve method (ICE-PIC) [52]. In the minimal-curvature-trajectory based approach, an optimization procedure is adopted for the generation of optimal low-dimensional manifolds or 1D trajectories [53]. The reduction and optimization method proposed in the present paper aims at the generation of reduced reaction mechanisms for hydrocarbon combustion which are able to capture ignition delay times over broad validity ranges, defined by engine-relevant conditions. In this case, the optimization procedure is not meant to reduce the number of species, but to optimize the reaction rate constants for selected reactions, ranging within the degree of uncertainty retrieved in literature data of the elementary reactions involved, especially for high order hydrocarbons. In particular, the most noticeable example of an optimized reaction mechanism is the GRI-mech for methane and hydrogen combustion [54, 55]. An automated optimization methodology for the reaction rate parameters has been proposed and applied by Elliot and coworkers to a reaction mechanism for an aviation fuel [17, 34, 56]. A novel approach was proposed for overcoming two possible issues arising during reduced mechanism preparation: on the one hand, the need for reducing as much as possible the dimensions of the mechanism may lead to unacceptable errors in the prediction of combustion profiles, especially as far as low temperature chemistry is concerned, thus leading to inaccurate predictions of ignition delay periods. The engineering strategy of fitting parameters to produce computationally-efficient extremely reduced one- or two-step schemes [57–59], also may be not suitable to model the combustion behaviour of complex and multicomponent fuels, and the consequent pollutant formation in practical combustion systems. On the other hand, mechanism optimization for a huge number of reaction rate parameters may require long computational times for reaching the optimum mechanism configuration.

3

1.2. Aim of the present work.

In this work a mechanism reduction and optimization procedure is set up to generate a skeletal mechanism of smaller size, which is still capable of giving detail at both low- and high-temperature chemistry, as well as at a broad range of pressures. This is meant to allow simulations of practical interest, such as regarding internal combustion engines, to be carried out including reliable chemistry in reduced computational times. The proposed methodology features an iterative algorithm, which carries out a progressive reduction in the number of species from the full mechanism, and the optimization of the relative reaction rate parameters at each iteration. It is shown that this procedure allows optimizations based on genetic algorithms (GA) to be performed under a rather limited number of merit function evaluations with fairly good results. The iterative procedure stops as soon as the reduced and optimized mechanism is not able to fit the requested error tolerances. The "optimum" solution identified at the end of the procedure is not simply the reduced mechanism which best fits the behaviour of the full one. Instead, a two-step optimization has been considered. The first step assures that the transient behaviour of the reduced mechanism fits the behaviour of the full one. The second step "optimizes" reaction rates, chosen within their own uncertainty ranges, to ensure that the final reduced mechanism best represents measured fuel oxidation behaviour through comparison with experimental data available in the literature. The second step is performed to account for uncertainties that are inherent in the full mechanism due to reaction rate estimations used on many of the reactions for which experimental data were not available. As an example, the procedure is applied to a well established mechanism for ethanol combustion, showing good reliability of the methodology, and the applicability of the reduced and optimized mechanism to cases of engine-like conditions.

In the following paragraphs, the reduction and optimization methodology is presented, together with its implementation in the iterative algorithm. Details are given on the development of a single-objective, GA-based optimizer for the calibration of the reaction rate parameters, and on the adoption of a suitable merit function formulation. Then, the aspects of the application of this procedure to the generation of a reduced mechanism for ethanol oxidation are presented and discussed. Finally, the results show the applicability of the reduced mechanism to both ignition delay predictions and engine simulations.

4

2. Methodology

The methodology herein proposed aims at generating a comprehensive reduced mechanism which is able, while considering the major reaction paths, to predict accurate combustion profiles at a variety of engine-relevant conditions. However, simply reducing the number of species and the reactions involving them can lead to inaccurate predictions of reduced combustion mechanisms, due to the lack of resolution in the representation of low-temperature chemistry [1]. Furthermore, sometimes the detailed mechanisms themselves are validated for limited ranges of pressures, temperatures and equivalence ratios, and their predictive capability can be weaker when simulating many practical combustion systems in which broad ranges of operating conditions are observed.

2.1. Mechanism reduction through an iterative procedure.

For these reasons, the present approach relies on the generation of a reduced combustion mechanism starting from an already established, detailed one. Then, as the number of species and reactions is reduced, the progressive loss of accuracy due to the elimination of the less important reaction paths needs to be compensated for. This can be accomplished by correcting the collision frequencies and activation energies of the reactions involving such hydrocarbons. This operation is not meant to generate artificial, unphysical reaction rates. Thus, the allowed ranges of variation of the reaction rate parameters were commensurate with the uncertainty associated with them in the literature. The aim is to account for the effects of the reaction paths which have been deleted in the surviving reactions. Thus, after analysis of the data in the NIST kinetics database [60], valid ranges for allowed variations of the Arrhenius parameters during the correction process were limited to $\pm 15\%$ for the activation energy, and $\pm 80\%$ for the collision frequency value. An iterative procedure was established, ruled by an error function formulation, which quantifies the deviation of the reduced mechanism from the detailed one. This kind of procedure can easily be automated, as all of its steps can be defined through analytical formulas and logical operators. The details of this procedure are represented in the form of a flow chart in Figure 1, while the methods defined and adopted for the mechanism reduction and optimization are discussed in the following paragraphs. In particular, a desired error tolerance for the reduced mechanism needs to be set. The iterative

5

procedure then starts from a first reduction in the number of species and reactions, with a high cut-off value for species deletion, so that a high number of species is retained in the reduced mechanism. Next, an error function is evaluated to check whether the reduced mechanism still behaves within the requested tolerance. In this case, the cutoff value is further reduced, so that a greater number of species – together with the reactions involving them – can be deleted from the mechanism. This progressive reduction of the dimensions of the reduced mechanism is continued until the error function value exceeds the maximum tolerance allowed. In this case, the reduced mechanism is corrected through the optimization of the Arrhenius parameters so that the effects of the reaction paths progressively excluded from it can be accounted for in the selected reactions from the remaining scheme. In case the optimum solution still fits the error tolerance requirements, a further reduction step can be pursued. Otherwise, the procedure restores the latest valid mechanism configuration.

Once these steps are completed, a reduced mechanism is generated, which behaves consistently with the detailed one. Then, the performance of the mechanism is compared to available experimental data, in order to have it fit the desired range of temperature and pressures. For this purpose a secondary optimization is carried out and a different error function formulation is adopted for quantifying the mean squared error, shown in terms of ignition delay predictions, and compared to available sets of experimental ignition delay measurements.

2.2. Definition of an error function for the reduced mechanism.

The definition of the error function for estimating the global error introduced in a reaction mechanism due to the elimination of less important species and reactions is mandatory, since the effectiveness of this indicator affects not only the possibility of finding the optimum reduced mechanism, but also the efficiency of the algorithms chosen for the mechanism reduction and optimization. In particular, some observations have been posed that define the requirements for the error formulation:

- The function should cover a broad range of operating conditions, as the reduction and optimization process aims at generating a mechanism which is valid over the broadest range of conditions occurring in practical combustion systems, and in particular in internal combustion engines. Particular relevance needs to be posed on lean conditions and
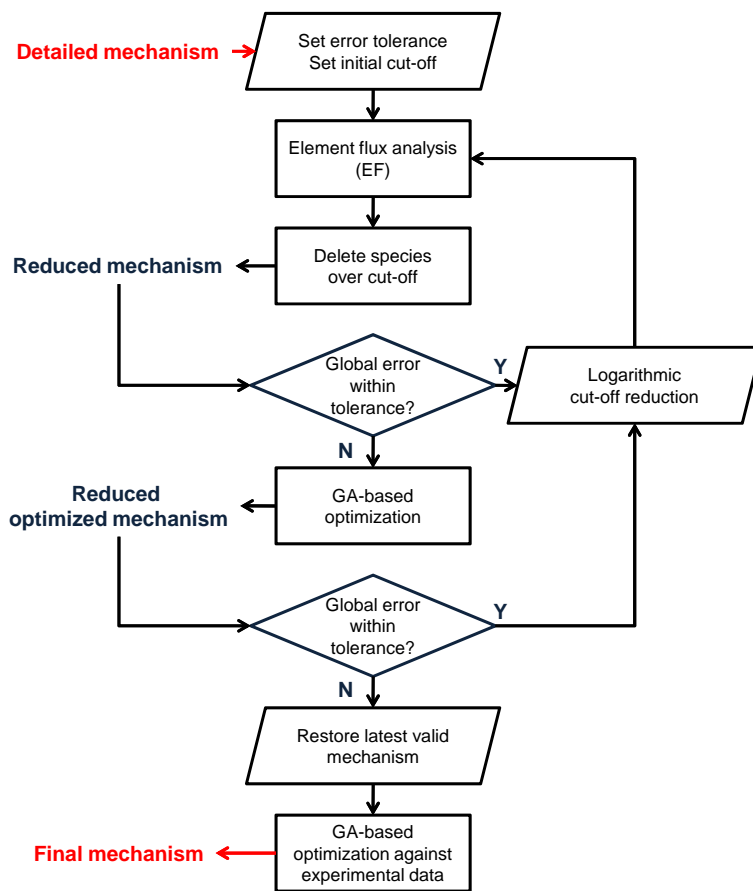
Figure 1: Flow chart of the procedure for mechanism reduction and optimization.

low temperatures, as it is acknowledged that the generation of reduced mechanisms affects low-temperature chemistry [1];

- The function should not vary by many orders of magnitude: genetic algorithms based on fitness-proportionate selection rely on the assumption that, when creating a new generation of individuals, the probability an individual has to be selected for reproduction is proportional to its fitness value. Thus, in case the best individual has a fitness value much higher than the others, it is likely that most of the next generation will be made with its chromosomes only, so that most of the genome of the previous generations are lost;

- The formulation of the error function should be valid both during the mechanism reduction procedure, and during the optimization phase. In the first case, the independent variables of the problem are binary, as they can be represented as the presence or absence of any reaction in the reduced mechanism. On the other hand, in the optimization problem all of the Arrhenius parameters can vary within a continuous validity range. Thus, the error function should not explicitly rely on these parameters, but should instead involve the actual physical behaviour of the mechanism.

As a reference for building an error function the formulation proposed by Elliot et al. [32] was chosen:

$$f = \left\{ 10^{-8} + \sum_{j=1}^{n_c} \sum_{k=1}^{n_s} W_k \frac{\left| X_{jk}^{calc} - X_{jk}^{orig} \right|}{X_{jk}^{orig}} \right\}^{-1}. \qquad (1)$$

In equation 1, a merit value for a modified mechanism is expressed through the comparison to the reference one. The merit value is higher as the model error is reduced. In order to estimate the model error, a sum of relative errors is made, which compares the final molar fractions X of all the n_s species in the mechanism after constant volume simulations over a set n_c of initial reactor conditions.

This formulation has proven to be suitable for the optimization of combustion mechanisms of large hydrocarbons [17, 34]. Moreover, it is able to account for important or unimportant species through a weighting factor W_k; however, it is not designed to take into account the time evolution of the species, and its value may be misleading in this case, where the optimization focuses not

only on the ignition delay time, but on the overall behaviour of the reduced mechanism. For this reason, it has been modified, and improved as follows:

$$f = -\log\left\{10^{-8} + \frac{1}{n_c\left(1 + \sum_k W_k\right)}\sum_{j=1}^{n_c}\left[\sum_{k=1}^{n_s}\int_{\tau=0}^{\tau=t_j} W_k\frac{\left|X_{jk}^{full}(\tau) - X_{jk}^{red}(\tau)\right|}{X_{jk}^{full}(\tau)}d\tau + \int_{\tau=0}^{\tau=t_j}\frac{\left|T_j^{full}(\tau) - T_j^{red}(\tau)\right|}{T_j^{full}(\tau)}d\tau\right]\right\}. \quad (2)$$

In particular, a total integration time t_j is defined for each of the reactor operating conditions, and needs to be estimated a priori; it has been chosen to add up to 1.5 times the mixture ignition delay period at the current conditions. Thus, the relative error from the comparison between the full and the reduced mechanisms is numerically integrated over the whole simulated time, for each of the n_c cases. A total of one thousand sampling points for the numerical integration was found to perform well. The weighting factor W_k is used not to give different weights to the species, but instead as a binary selector for the species to either be included or not in the error function computation. Furthermore, an error analysis on temperature profiles T_j has been added similar to the approach proposed by Banerjee and Ierapetritou [18], as global heat release is one of the key quantities for defining the effectiveness of the reaction mechanism. Finally, the logarithm operator is considered, as the error function derived from the integration of the relative errors of the species profiles can vary many orders of magnitude. Applying the logarithm implies that the resulting values of f remain of the order of unity and thus are particularly suitable for GA-based optimization.

The choice of the operating conditions to be simulated for defining the reduced model's error function is problem-dependent. However, the whole set is intended to cover the range of operating points that the mechanism is developed for. The choice of a small number of points, or of a narrow space will eventually lead to a mechanism with a limited validity range. More details for the 18 operating points chosen in the present analysis for the ethanol combustion mechanism are given in the following.

Finally, the following set of species to be monitored has been assumed:

$$N_s = \{fuel, O_2, OH, HO_2\}. \quad (3)$$

Apart from fuel and oxidizer, OH and HO_2 radicals have been chosen due to their well acknowledged importance in slow hydrocarbon oxidation and ignition delay timing [61, 62]. Despite the possibility to consider the whole set of species in the

9

reduced mechanism, the choice to keep a unique species kernel for the error cost function has been adopted for assuring consistency of the results of the reduction procedure over various mechanism sizes; also, this allowed to focus on the ignition characteristics of the mechanism, as wider subsets would have eventually led to give importance to species which were likely to be removed during the next steps of the reduction procedure.

Finally, this general formulation of the merit function would allow the same approach to be also applied to a spatial distribution more than a time integration, for instance in case some experimental measurements of laminar flames are available in terms of temperature and species mass fraction profiles. However, the sensitivity of these computations to the initial conditions makes this approach less suitable to an automatic casefile generation as required by a genetic-algorithm-based optimization.

2.3. Species reduction through element flux analysis (EF).

Among the methodologies for the analysis of species activity in reaction mechanisms, Element flux analysis (EF) is based on the assumption that the instantaneous reactivity of the species across all the reactions can be quantified by the fluxes of atoms of selected elements. This method, first introduced by Revel et al. in 1994 [30], has also been proposed by Androulakis et al. [16] as a tool for identifying the the contributions of species in detailed reaction mechanisms over an integrated time interval. More recently, He, Ierapetritou and Androulakis have improved the methodology and shown the potential of this approach as an efficient pointer for quantifying the instantaneous reactivity of the species. In some recent papers, [14, 21, 22] they have adopted element flux analysis to identify reaction pathways, and to develop reduced mechanisms on-the-fly both in batch reactor and in CFD combustion simulations.

The core of the EF analysis is the definition of an instantaneous flux pointer $\dot{A}_{ijk}$, which quantifies the flux of atom A, in the i-th reaction, from the species with index j to the one with index k:

$$\dot{A}_{ijk}(t) = (|q_{f,i}(t)| + |q_{b,i}(t)|) \frac{n_{A,j} \, n_{A,k}}{N_{A,i}}, \qquad (4)$$

where $n_{A,j}$ represents the number of atoms of element A in species j, and $N_{A,i}$ the total number of atoms of the element involved in the whole reaction i. He et al. have improved the original formulation by Revel et al. by explicitly separating the original term for the reaction progress variable, q_i, into the sum of two absolute values, cumulatively accounting for the forward and backward atom fluxes within the same reaction. This assumption is motivated by the need to prevent the atom fluxes of reactions near equilibrium from being evaluated as negligible.

In our approach, the element flux analysis is the basis for mechanism reduction, as it is meant to provide an index of the importance the species play across the whole ranges of validity the mechanism is intended for. Thus, the concept of flux time-integration introduced by Androulakis et al. [16] has been modified into:

$$A_{jk} = \sum_{c=1}^{n_c} \left\{ \int_{\tau=0}^{\tau=t_c} \left[\sum_{i=1}^{n_r} \dot{A}_{ijk,c}(\tau) \right] d\tau \right\}; \tag{5}$$

the overall flux indicator A_{jk}, for the species source-sink pair (j,k), is thus numerically integrated over the simulated time, and summed over the whole set of mechanism operating points n_c chosen for defining its desired validity range. The total flux of element A exchanged during the whole set of simulations is evaluated taking into account all the possible source-sink pairs, represented by the cartesian product of the species array with itself:

$$A_t = \sum_{j,k \in N_s \times N_s} A_{jk}. \tag{6}$$

The species selection is then made upon the analysis of the contribution of the element fluxes A_{jk} to the total flux A_t. The element fluxes are first sorted in decreasing order, and a cut-off value $c \in [0.0, 1.0]$ represents the fraction of total element flux chosen to be accounted for in the reduced mechanism. Only the species involved in the fluxes at the first n positions of the sorted flux array, n defined as the minimum number of positions for which the cumulative sum of their values reaches the total flux threshold, is retained in the reduced mechanism.

As an example to clarify this assumption, in Figure 2 the results of the EF analysis performed on an ethanol combustion mechanism [8] – used as a test in the present study – are presented. The sum of the element fluxes for carbon and oxygen atoms are plotted for each of the species contributing to the cutoff value. The values are normalised against the sum of the total exchanged element fluxes, as in Eq. 6. The figure shows that the species which participate less to the total element fluxes are more likely to be deleted, as the cutoff value is decreased. For example, in the figure two different cutoffs – 99.9% and 99.0% of the total amount, respectively – are compared. The resulting selected numbers of species, having positive normalized contribution to the element flux, adds up to $n_s = 55$ and $n_s = 50$. A fixed contribution, equal to 1.0, is set to the whole set of species of the O-H system, which is assumed to always be present in every reduced combustion mechanism.

In the present mechanism reduction procedure, as illustrated in Figure 1, the EF analysis is called at each iterative step with a different cutoff value, in order to achieve the progressive deletion of the less important species. The initial cutoff

11
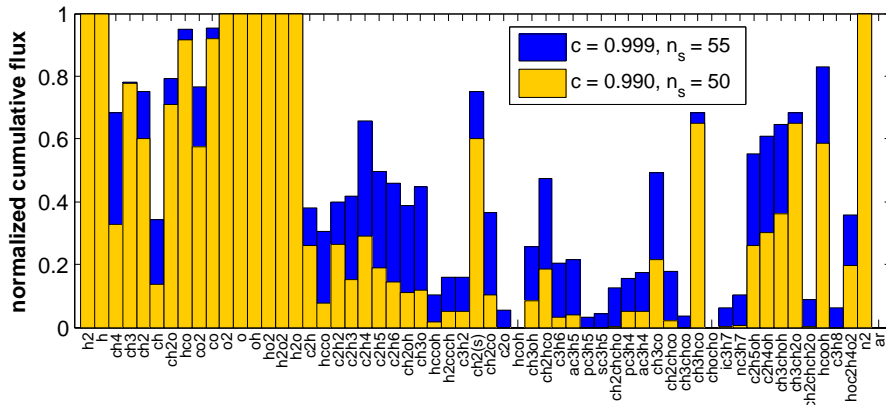
Figure 2: Species selection through EF analysis for an ethanol combustion mechanism [8]: normalized cumulative fluxes for carbon and oxygen atoms over 18 operating conditions. Cut-off values: $c = 0.999$ and $c = 0.990$.

value is set at $c = 99.9\%$, and at each following step it is decreased following a power law: $c(n + 1) = c(n)^{1.1}$. This choice is motivated by the fact that, during the first optimization steps, the reduced mechanism still consists of a huge number of reactions: the number of variables to be optimized is high, thus either requiring unacceptably high computational times to carry on the optimization, or leading to a non negligible probability that the GA-based optimizer will not find the optimum solution in case a limited numbers of evolutionary steps and a narrow population size is considered.

2.4. Mechanism correction: GA-based optimization.

2.4.1. Genetic algorithms and chemical kinetics.

The adoption of genetic algorithms for efficient single- and multiple-objective optimization is appealing, due to its effectiveness in getting the solution of the optimization problem, and the relatively small number of function evaluations required [63]. There is evidence in the literature concerning the use of genetic algorithms for the development of combustion mechanisms. GA has been used for the generation of reduced combustion mechanisms setting an optimization problem to be the choice of species and reactions [15, 64]: Banerjee and Ierapetritou [18] for example show the effectiveness of the genetic algorithm in choosing a reduced set of species and reactions from a detailed mechanism, exploiting the binary representation of chromosomes in the evolutionary algorithm, which allows the presence or absence of an item of the original set to be represented throughout the two possible instances – namely 0, or 1 – of its corresponding allele. Reduced mechanisms achieved through

this approach can reach very small dimensions, even if their validity range is limited, and thus a set of reduced mechanisms may be needed for covering the range of operating conditions in practical combustion systems. The method has been used for the development of a unique reduced mechanism, for example when applied to HCCI engine multidimensional simulations. Montgomery et al. [65] have shown that the integration of GA-based optimization into the selection of quasi-steady-state (QSS) species can dramatically improve the procedure. Furthermore, application of the GA technique in terms of reduction in the number of reactions for the development of reduced mechanisms for engine-relevant conditions has been shown to be viable for reductions in the dimension of the original mechanism [66]. A second possible application of GA-based optimization is in the search for optimal values of reaction rates. Among the first examples of this second approach, Hamosfakidis and Reitz adopted a genetic algorithm for calibrating a simplified ignition model for a diesel fuel surrogate [67]. In this work, the optimization featured a total of 26 independent variables, and an impressive improvement in the ignition model performance was achieved over a broad range of operating conditions. As far as full combustion mechanisms are concerned, an extensive review on this approach is given by Elliott et al. [32]. They showed that the adoption of genetic algorithms can be very efficient in tuning the reaction rate constants, as the large number of variables involved makes this implementation more suitable than analytical optimization methods. Since most reaction rates for high-order reactions, such those involving large hydrocarbons still are not well established, Elliot et al. [56] suggested that the validity ranges for the independent variables should be chosen to fit the degree of experimental uncertainty given by the data available for the reaction. The most complete collection of reaction rates was provided by the NIST kinetics database [60].

This methodology may require prohibitive CPU times for optimization of mechanisms for large hydrocarbons, and the same authors have more recently developed a novel approach, based on a two-step genetic optimization [17, 34]. In the first step, the optimization aims at reducing the number of species. The chromosome is a binary string with a number of alleles equal to the number of species in the full mechanism. The total number of active species is kept fixed and equal to the number of species chosen for the reduced mechanism and the merit function is based on the performance of the reduced mechanism, in comparison with the full one. Once the reduced set of species is gathered, a second optimization step is carried out in order to tune the Arrhenius reaction rate parameters, A_i, b_i and E_i, $i = 1, ..., n_s$. In the present work, GA-based optimization is nested into the iterative procedure. The reduction in the number of species is treated through the element flux analysis, while the GA is run only for the calibration of the reaction rate parameters. As the number of species is progressively reduced at each iteration, an optimization on the

reaction rate parameters of the reduced mechanism is carried out, when the error function of the reduced mechanism exceeds a desired tolerance value. This choice is motivated by two reasons: the need for reducing the total computational time, and the fact that our reduction and optimization approach is ruled by a constraint on the performance of the reduced mechanism, aiming to get as few species as possible.

2.4.2. Optimization problem definition.

Forward reaction rates in common reaction mechanisms are mostly computed according to the Arrhenius formulation, which features three parameters needed for defining the behaviour of each reaction [68]:

$$k_{f,i} = A_i \, T^{b_i} \, \exp\left(\frac{E_i}{R\,T}\right), \qquad i \in \{1, ..., n_r\} \,. \tag{7}$$

In case the mechanism features more complex reactions, such as pressure-dependent ones, more complex formulations are usually adopted; for example, in the CHEMKIN library [69] the Troe and SRI forms are allowed [70, 71], in which two Arrhenius-like reaction rates are defined at the low and high pressure limits, plus a number of parameters are needed for computing the pressure-dependent behaviour. Lastly, in practical combustion mechanisms, reverse reaction rate calculation through the equilibrium theory is sometimes overridden by a further explicit Arrhenius-like formulation, which adds three parameters to the reaction definition.

In this work, the optimization problem is approached defining a fixed number of independent variables, twice the number of reactions to be optimized. In particular, only the collision frequency value A_i and the activation energy E_i are optimized. The choice not to include the temperature exponent b_i is motivated by the fact that most temperature exponents in the reactions are zero [1].

Not all of the reactions in the combustion mechanism need to be tuned: as a matter of fact, reaction rates for most of the reactions involving low-order schemes, such as the elementary oxygen - hydrogen system are well established. For this reason, the optimization problem is set not to address the reaction rate coefficients of reactions involving only species within the following set:

$$N_{basic} = \{H, H_2, O, O_2, OH, H_2O, HO_2, H_2O_2, N_2, CO, CO_2\} \,. \tag{8}$$

The reaction rates of all reactions which involve at least one species not in the set N_{basic} are thus optimized. Two reaction rate parameters, A_i and E_i thus need to be identified not only for elementary reactions with an Arrhenius formulation, but also for reactions with an explicit reverse reaction rate expression, as well as pressure dependent reactions. In the first case, assuming an explicit reverse rate

14

expression leads to an 'effective' equilibrium constant which is different from the value computed through minimization of the reaction free energy. In our approach, no actions are taken in order to change this assumption, and, in case such a formulation is found in a detailed mechanism, the independent variables still remain the two forward reaction rate parameters; the explicit reverse reaction rate constants are accordingly modified, in order to maintain the modified equilibrium constant as arising from the original mechanism:

$$A'_{r,i} = A^0_{r,i} \, A'_{f,i}/A^0_{f,i}; \tag{9}$$

$$E'_{r,i} = E^0_{r,i} + \left(E'_{f,i} - E^0_{f,i} \right). \tag{10}$$

In the second case, two Arrhenius-like formulations describe the reaction rates at the high and low pressure limits. The reaction rate parameters at the high pressure limit are considered as independent variables for the optimization.

Once that a unique definition of the set of independent variables is obtained, the allowed validity ranges of the variables need to be defined. In our approach, a fixed validity interval is set for each of the variables, centered on the previous value from the original mechanism, and with fixed width: $A_i \in \left[A^0_i - \Delta A_i; A^0_i + \Delta A_i\right]$; $E_i \in \left[E^0_i - \Delta E_i; E^0_i + \Delta E_i\right]$. The two range bounds adopted during the optimizations were $\epsilon_A = \Delta A_i/A_i = 80\%$ and $\epsilon_E = \Delta E_i/E_i = 15\%$. The adoption of these two average values was found after a comparison of experimental reaction rates retrieved from the NIST chemical kinetics database [60]. The average uncertainty ranges which affected reaction rates involving C1-C3 hydrocarbons were chosen as a reference for fitting the optimization ranges. This choice is problem-dependent, and has been motivated by the fact that the following optimization has been applied to an Ethanol combustion mechanism which includes many hydrocarbon species of those sizes. As an example, Figure 3 shows the comparison among different values of the reaction rate parameters for the decomposition of propene into methyl and vinyl radicals. Here, range bounds defined by the aforementioned delta are applied to the values present in the ethanol combustion mechanism from Marinov [8]. The two bands are able to correctly cover all the values reached by the other formulations for the same reaction. It is clear that the choice of assuming average validity intervals with fixed percentage allowance may not fit the data uncertainty for each of the reactions, and that, in order to preserve the physical soundness of this assumption, a further analysis would be required in case of mechanisms featuring larger hydrocarbons or different species. Nevertheless, this procedure is particularly suitable for implementation in an iterative algorithm, while detailed estimation of these bounds for each of the reactions in the full mechanism would need a large pre-processing effort, which is beyond the scope of the approach.
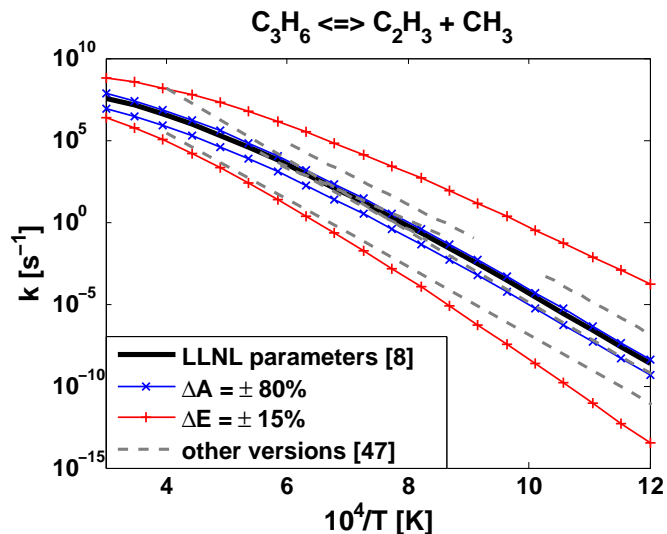
Figure 3: Comparison among different forward reaction rate constant sets for reaction $C_3H_6 <=> CH_3 + C_2H_3$. Reaction data from LLNL ethanol combustion mechanism [8] and NIST kinetics database [60].

In order to complete the definition of the optimization problem, once the function to be evaluated and the independent variables and their validity ranges have been identified, the solver for the GA-based optimization needs to be set up as described in the following paragraph.

2.4.3. The GA-based optimizer.

In order to carry out the optimization problem described above, a code for the optimization of reaction rate constants was developed, based on an evolutionary algorithm [72]. The optimizer features a single-objective, binary-coded genetic algorithm, where an initial population of individuals is generated, and then let to evolve for a number of generations following the principles of natural selection operators, such as reproduction, mutation, and crossover. Each individual is represented by a set of binary strings, namely chromosomes, which stand for the values of the independent variables to be optimized. The binary representation implies thus that the validity ranges of the variables have to be discretized into a finite number of divisions. If the range is defined by the continuous interval $[v_{min}, v_{max}]$, this is spanned through chromosome instances ranging from $v_{min} = 00...0$ to $v_{max} = 11...1$, and the total number of divisions, 2^{n_g}, is set by the number of digits – or genes –, n_g, of the chromosome itself. The total number of possible solutions (each of the

16

variables has the same chromosome length) is thus given by $2^{n_g \cdot n_v}$, where n_v is the total number of variables. n_v can add up to thousands. Thus, when optimising reaction rate parameters, a three bit chromosome length $n_g = 3$ has been chosen, fixed for each variable, resulting in eight subdivisions of the validity interval. Each chromosome is assigned a merit value, computed through the evaluation of the fitness function, defined in Eq. 2, as a result of a set of constant pressure calculations. Each new generation is evolved from the previous one as the three operators of the genetic algorithm are applied. *Fitness-proportionate selection* of the individuals is the main operator affecting reproduction. Each of the new individuals appearing in the new generation has two parents, which are selected randomly from the previous one. The random process is however biased, as the probability that each individual is selected is proportional to its fitness value [63]. A *mutation* operator, occurring after reproduction with a fixed probability, introduces new combinations in the genotype by inverting a randomly chosen gene within the chromosome. *Crossover* is a recombination operator which cuts the chromosomes of the two parents at a random locus, and exchanges the two cut parts between them. In particular, the iterative procedure adopted in the present GA for simulating the evolution of the population can be schematised as follows:

1. Generation of the first population: N_p individuals, consisting of randomly generated chromosomes.
2. Evaluation of the fitness function for each of the individuals.
3. Fitness-proportionate selection of $f_R \cdot N_p$ couples of individuals for reproduction.
4. Reproduction of the individuals: each chromosome randomly chosen from one of the parents.
5. Possible occurrence of mutation and crossover, with p_M and p_C probabilities.
6. Substitution of the $f_R \cdot N_p$ worse individuals with the newly generated ones. Begin a new generation.
7. Evaluation of the fitness function for each of the new individuals.
8. Go to 3.

The parameters ruling the GA operation are summarized in Table 1. Most of the parameters follow the guidelines suggested by Mitchell [63]. The GA is normally iterated up to 50 to 500 generations; and the population size is made up of 5 to 50 individuals. An exception has been considered for the mutation probability, which is to be kept very small ($p_M < 0.01$). In this case, however, it is necessary to introduce a high degree of randomness due to the fact that the population size scarcely allows the whole variable space to be covered, and having a high probability of mutation allows zones which are not present in the first generation

17

to be gradually introduced during the optimization process. The reproduction fraction is chosen at 90% as it is acknowledged that keeping only few, near-optimum individuals from one generation to the next can improve the algorithm convergence; crossover probability is the recommended value.

Parameter	symbol	value
number of individuals	N_p	75
number of generations	N_g	200
chromosome length	n_g	3
reproduction fraction	f_R	0.90
mutation probability	p_M	0.60
crossover probability	p_C	0.35

Table 1: Parameters setting the genetic optimizer.

3. Results and discussion

3.1. Reduction of an Ethanol combustion mechanism

The methodology was tested through the development of a reduced mechanism for ethanol oxidation. As a starting mechanism for the reduction and optimization procedure, the mechanism developed by Marinov [8] was chosen. This mechanism consists of 58 species and 383 reactions, and has been validated against experimental data for high temperature oxidation (T > 1000K). In order to test the reliability of the reduction approach, a broader set of temperatures and equivalence ratios was chosen to define the validity range of the new mechanism. In particular, cases of interest to internal combustion engine simulations were chosen, resulting in a total of 18 different initial conditions with pressure values $p_0 \in \{2.0; 20.0\}\, bar$; mixture equivalence ratios $\phi_0 \in \{0.5; 1.0; 2.0\}$; temperatures $T_0 \in \{750; 1000; 1500\}\, K$. This set of operating conditions was kept fixed during the whole reduction and optimization procedure. Integration times for the constant pressure reactors were found for each of the cases after proper analysis, and set equal to 1.5 times the ignition delay period, where the ignition delay is defined as the time needed by the system to reach a 200K increase in temperature. Each of the integration intervals was then subdivided into a set of one thousand equally-spaced observation points for the following evaluation of the accuracy of the reduced mechanisms.
The reduction and optimization algorithm was then run setting an error tolerance in terms of a merit function value. The condition for carrying out a further reduction without the need for optimizing the Arrhenius parameters was set at $f > 3$, corresponding to a cumulative relative error – summed over the 18 cases

18

(hence, 18000 observation points) – to be less than $5.0e-2$. The second part of the optimization, aimed at the calibration of the reduced mechanism against experimental ignition delay measurements, was run instead considering a different set of initial conditions, also spanning the range of available data. The measurements by Curran et al. [73] were used for dilute ethanol oxidation at stoichiometric equivalence ratio ($C_2H_5OH = 2.5\%, O_2 = 7.5\%$), at three different pressure values $p_0 = \{2.0, 3.0, 4.5\}\, bar$. For each pressure level, 20 different initial temperature conditions were considered, logarithmically spanning the range between 1100K and 1500K. Furthermore, the merit function was defined using the reciprocal of the global error, computed as the cumulative sum of the least squares comparisons between the simulated and experimental data over the three pressure levels considered.

The last successful iteration of the algorithmic procedure generated a final reduced and optimized mechanism consisting of 33 species and 155 reactions. The overall computational time required was of about 9 hours on a personal computer running on a Core i7 860 CPU. The complete reaction scheme achieved is reported in the appendix Appendix A. During the run, the algorithm performed a total of 9 mechanism reductions through element flux analysis, two genetic optimizations for calibration on the original LLNL mechanism, and one GA-based optimization for mechanism calibration against experimental ignition delay measurements. In order to show the effectiveness of the methodology, the following comparisons consider the three versions of the skeletal reaction mechanism at the last successful reduction iteration, i.e. that considering a subset of 33 species and 155 reactions. The first version of the skeletal mechanism ("R") is the one generated after simple shrinking of the LLNL mechanism to the subset of species selected through element flux analysis; the second version ("RO") is the one having optimized reaction rate parameters after comparison with the detailed mechanism, according to the merit function in Eq. 2; the last version ("ROO") is that further optimized against the experimental ignition delay measurements from Curran et al. [73]. The acronyms adopted and the differences among them are summarized in Table 2.

Acronym	n_s	n_r	details
LLNL	58	383	Marinov, 1999 [8]
R	33	155	EF-analysis reduced only
RO	33	155	Reduced and optimized against LLNL
ROO	33	155	RO optimized against Curran, 1992 data [73]

Table 2: Description of the starting ethanol oxidation mechanism, and of the three reduced ones.

Figure 4 shows the full comparison among mechanisms LLNL, R and RO at the eighteen initial conditions considered. For the sake of simplicity only the temperature traces have been plotted, since they well represent the overall behaviour of the mechanism. In particular, it is observed that the simple reduction in the number of species through EF analysis cannot fit the broad range of operating conditions. As a matter of fact, the behaviour of mechanism R is never similar to that of the original mechanism, and it is closer to it only at low initial temperatures and low pressures. The optimized mechanism RO provides similar behaviour to that of the Livermore mechanism, where an excellent agreement is found especially at low initial temperatures. Furthermore, the predictiveness of the mechanism seems not to be affected by the change in pressure.

Figure 5 shows the history of the optimization ended in the generation of the RO mechanism: the optimum individual has an overall merit value $f = 18.532$, while the R mechanism, from which the GA-based optimization started, had $f = 2.678$; the maximum in merit value having been found by the genetic optimizer at generation 197. Values for the Arrhenius parameters of collision frequencies and activation energies are in the optimum mechanism different for each reaction, except for the set of reactions involving the basic species set as previously defined. In order to compare the values of the optimized RO mechanism with those of the reduced one, R, Figure 6 plots the relative variations of collision frequencies and activation energies in terms of relative differences, $\varepsilon_r(A_i) = \left(A_i^{RO} - A_i^R \right)/A_i^R$ and $\varepsilon_r(E_i) = \left(E_i^{RO} - E_i^R \right)/E_i^R$. In particular, the variation in Arrhenius parameters reached the bounds of the collision frequency for 27.7% of the reactions, and of the activation energy for 10.2% of the reactions, showing that the optimum values led to a new mechanism whose parameters were close to those of the original. The average variation in the collision frequency was $\overline{\Delta A} = 22.86\%$, and $\overline{\Delta E} = 4.29\%$ the average variation in activation energies.

The results of the second optimization process are summarized in Figure 7. The comparison between LLNL and RO mechanisms shows that both mechanisms suffer a slight overestimation of the ignition delays especially at the lowest initial temperature values. The generation of the ROO mechanism, optimized with the available set of experimental data, plotted in Figure 7 b), shows that this overestimation is completely solved after the optimization procedure.

As far as the computational costs of the procedure are concerned, the two contributions due to the iterative reduction procedure and due to the mechanism optimization phases have been considered. As acknowledged [1], the ODE integration of chemically reacting systems scales as n_s^3, due to most computational time being spent in evaluating the Jacobian matrix. Thus, the genetic optimization procedures have roughly been approximated as scaling with $n_{s,i}^3$, $n_{s,i}$ being the current
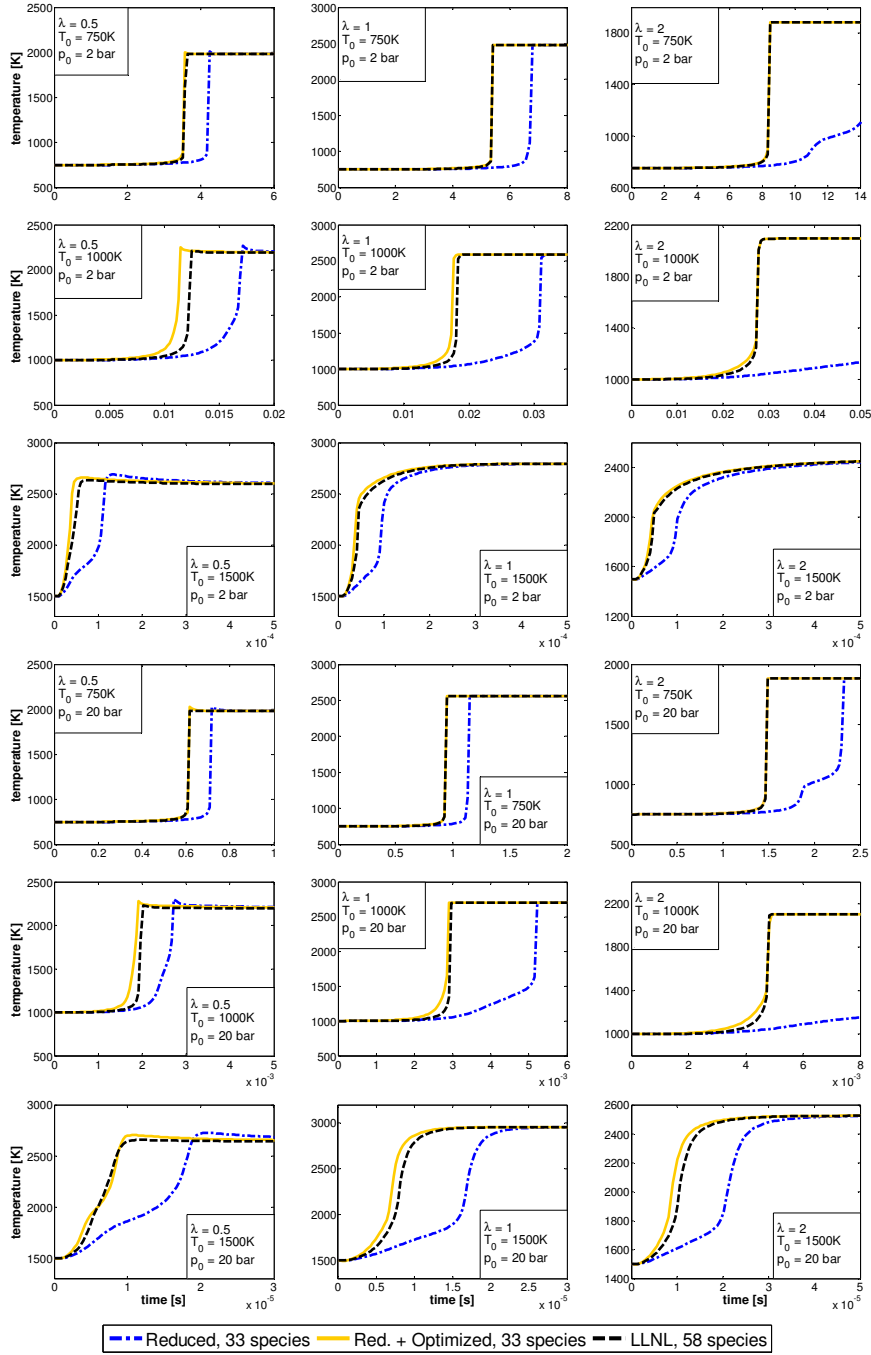
Figure 4: Temperature profiles simulated at the 18 operating conditions chosen for ethanol mechanism reduction. Comparison among LLNL, R and RO mechanisms.
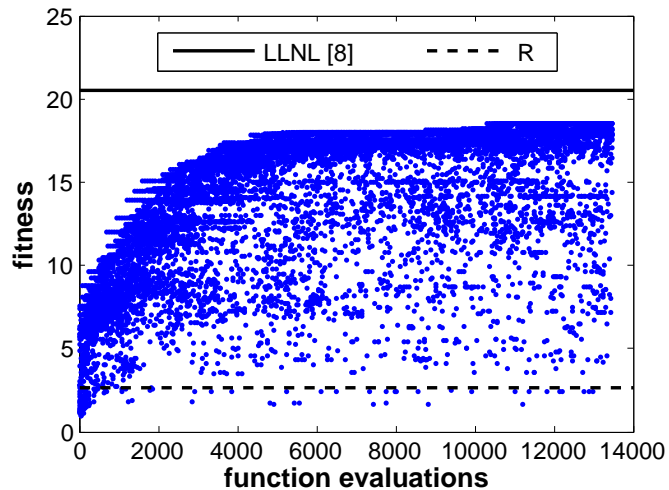
Figure 5: Evolution of the individuals' merit value during GA-based optimization over the 33 species, 155 reactions reduced mechanism.
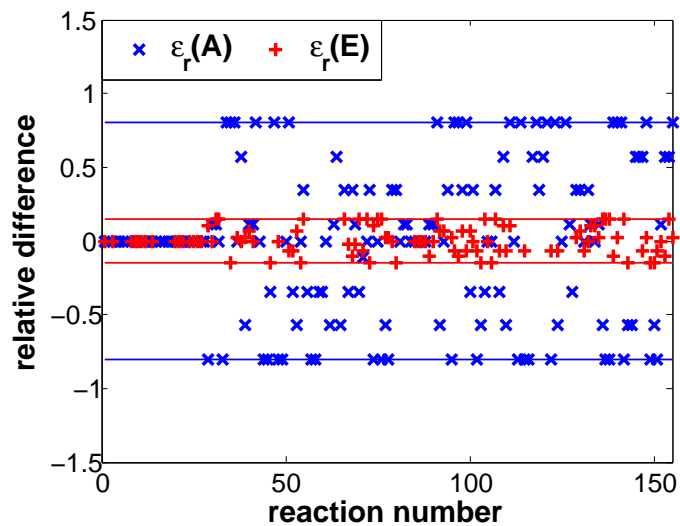
Figure 6: Relative differences of the optimized Arrhenius parameters in mechanism RO, in comparison with constants in the original LLNL mechanism [8].

22
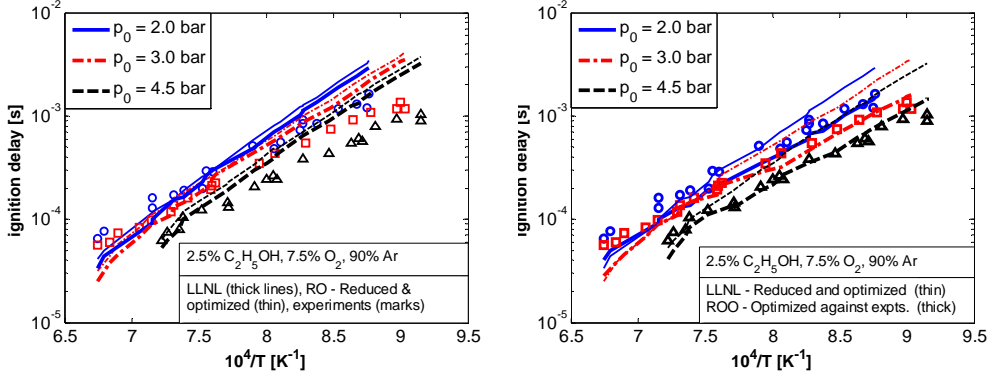
Figure 7: Comparison among predicted and experimental [73] ignition delays for dilute stoichiometric ethanol-oxygen mixtures. a) Left: comparison between LLNL and RO mechanisms; b) Right: comparison between LLNL and ROO mechanisms.

reaction mechanism size. The overall computational cost of the iterative procedure then scales with the total number of reduction-and-optimization iterations. From an analysis of the series of mechanism sizes as produced by the EF method, when applying the power law for cut-off value modification previously explained, mechanisms were seen to almost logarithmically decrease in size (as reported in Figure 8). Thus, if the same final reduced mechanism size is referred to, the overall number of iterations of the procedure roughly scales with $\log n_{s,1}$, $n_{s,1}$ being the dimension of the starting full mechanism. Thus, the average computational cost of the mechanism reduction and optimization methodology scales as $n_{s,1}^3 \log n_{s,1}$.

3.2. Application to HCCI engine simulations

As evidence of the predictive capability of the reduced mechanism, it was applied for modeling the combustion of an ethanol-air mixture in a HCCI-operated internal combustion engine. The simulation model is a zero-dimensional, adiabatic, single-cylinder HCCI research engine, with 14:1 compression ratio, running at 1200 rpm. Detailed specifications of the slider-crank mechanism can be found in [74]. Two baseline cases were considered, both at initial mixture equivalence ratio $\phi = 0.4$, and with different initial temperatures, $T_0 = 437K$ and $T_0 = 424K$. These reference conditions correspond to the Sandia experiments. Figures 9 and 10 show the comparison among the 4 mechanisms – namely, full Livermore (LLNL), EF-reduced (R), reduced and optimized (RO), optimized against experimental ignition delays (ROO) – in terms of pressure history, plus histories of the most important species. Figure 9 shows good agreement between the full Livermore's mechanism and the reduced and optimized one, while the simple reduction based
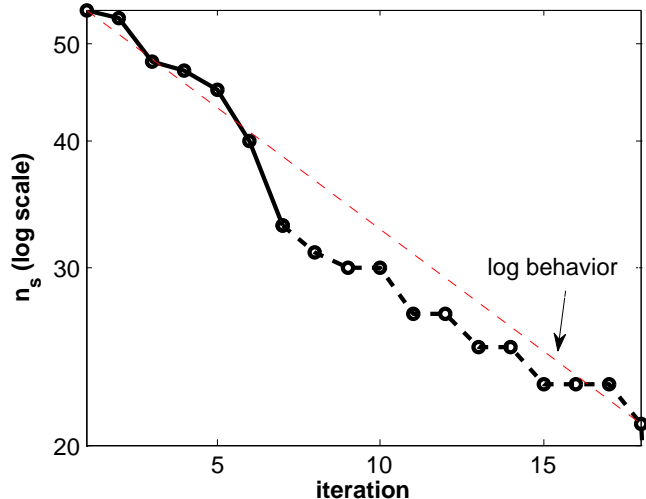
Figure 8: Reduction iterations for the Ethanol mechanism described in the following, and comparison with fully logarithmic behaviour. Total number of acceptable reduced mechanisms generated: 7.

on EF analysis fails to predict mixture ignition at these conditions. Concerning the ROO mechanism, it shows slightly earlier mixture ignition, in agreement with the results of the final optimization where the ignition delay predictions tended to earlier ignition especially when starting from the lowest temperature values. Similar behaviour is observed in the $T_0 = 424K$ case, as in Figure 10. Only the LLNL mechanism shows a different behaviour across the two cases: it fails to predict mixture ignition at the conditions with lower initial mixture temperature. The two reduced and optimized mechanisms showed less dependence on the initial mixture temperature, as the ignition delays predicted were consistent with those observed in Figure 9.

Figure 11 displays the behaviour of the mechanisms when doubling the in-cylinder pressure at intake valve closure. The same two initial temperature values as in the baseline cases were considered. Here, all the mechanisms show consistent behaviour. The LLNL mechanism is able to predict ignition even at the lower initial temperature, thus showing the mechanism's sensitivity to pressure; the R mechanism still is not able to predict ignition at both temperatures. In Figure 12, the first baseline case ($T_0 = 437K$) is operated with equivalence ratios leaner – $\phi_0 = 0.25$ – and richer – $\phi_0 = 0.70$ – than the original case. The same behaviour seen in the two baseline cases is observed, proving that the mechanisms show less depen-

24
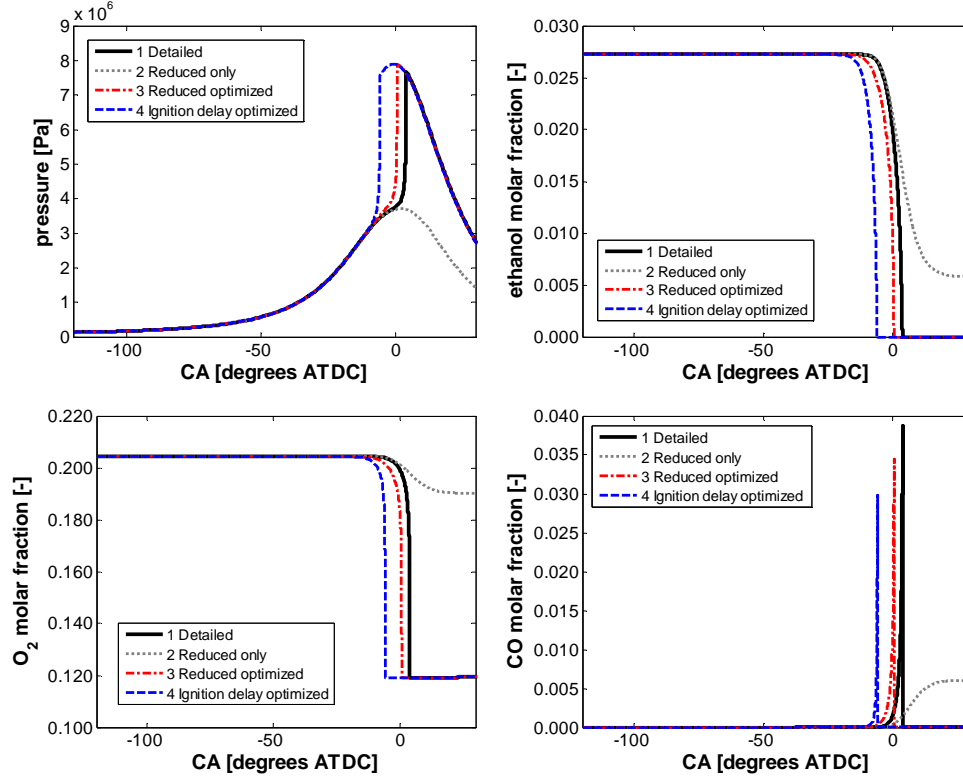
Figure 9: Simulation of baseline case 1 for the HCCI Sandia engine [74]: $\phi_0 = 0.40$, $T_0 = 437K$.

dence on mixture composition than on temperature and pressure. Finally, Figure 13 shows the results of multidimensional simulations carried out using the KIVA-4 code [75] coupled with detailed chemistry. The simulations have again been carried out using the four different mechanism versions, and compared with experimental average in-cylinder pressure curves: while most mechanisms tend to fail predicting mixture ignition, the ROO mechanism agrees well with the experiments at both cases. The good agreement at the two baseline cases has been confirmed also when sweeping the charge conditions at intake valve closing, as shown in Figure 14: the comparison between KIVA4 calculations and experimental measurements featured a set of in-cylinder pressure curves at varying boost pressure, and 50% total-heat-release crank angle values (CA50) at varying intake mixture temperatures. The results show that the reduced mechanism is able to correctly predict the combustion behaviour also at a range of engine operating conditions.
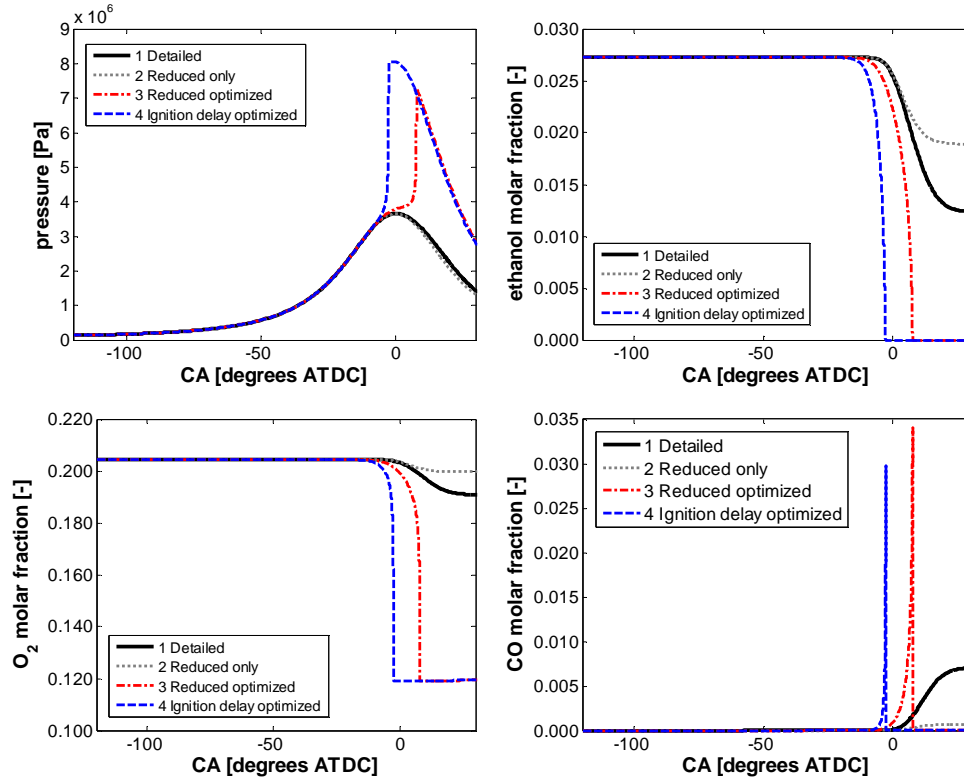
Figure 10: Simulation of baseline case 2 for the HCCI Sandia engine [74]: $\phi_0 = 0.40$, $T_0 = 424K$.
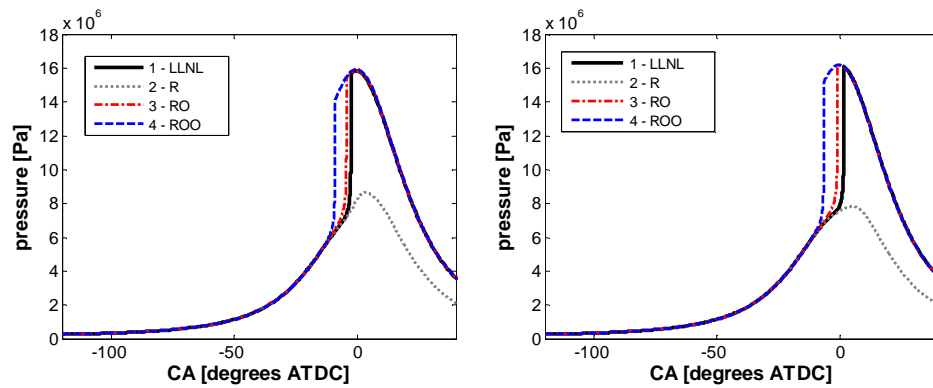
Figure 11: Simulation of the HCCI cases with doubled IVC pressure; initial temperatures: 437K (left), 424K (right).
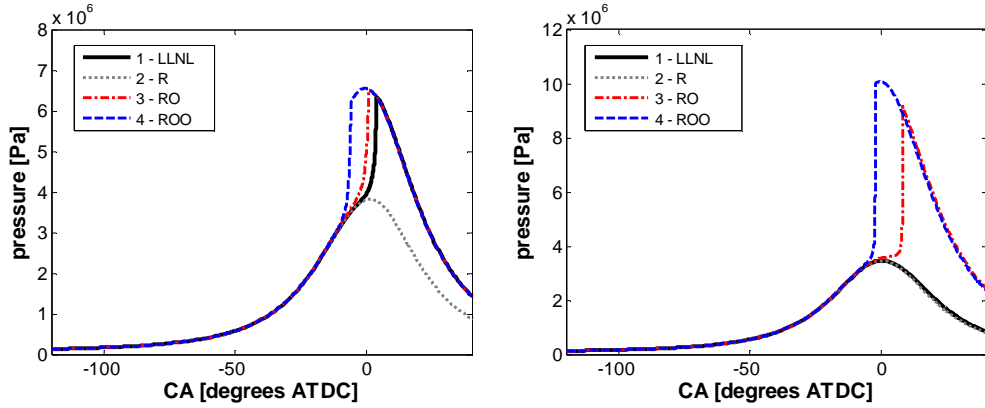
Figure 12: Simulation of the baseline HCCI case 1 with modified mixture equivalence ratios: $\phi = 0.25$ (left) and $\phi = 0.70$ (right).
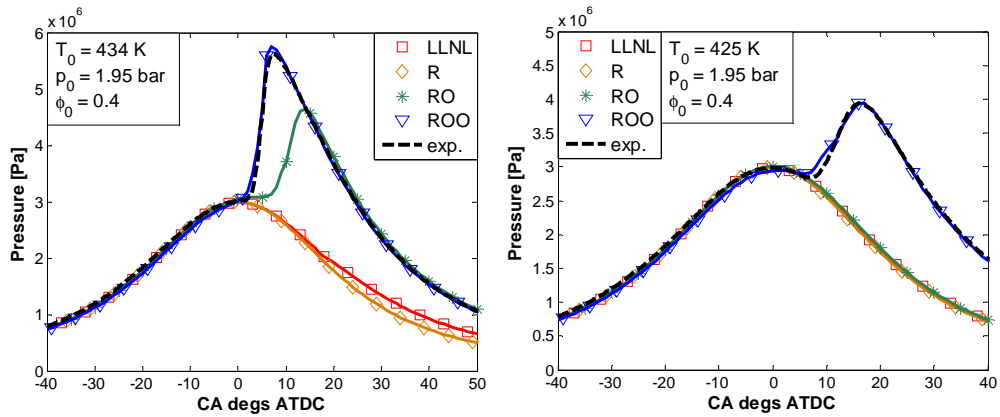
Figure 13: Comparison between multidimensional simulations and experimental data about the two baseline cases considered.
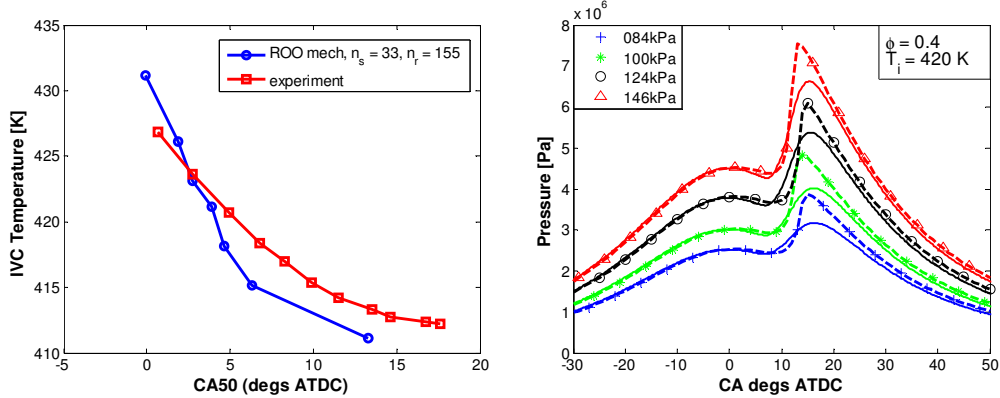
Figure 14: Left: experimental vs. numerical comparison of CA50 at varying IVC mixture temperatures. $p_{IVC} = 0.92bar$, $\phi = 0.4$. Right: Boost pressure sweep, from $p_{IVC} = 0.84bar$ to $p_{IVC} = 1.46bar$. $T_{IVC} = 420K$, $\phi = 0.4$. Solid lines: experiments; dashed lines and symbols: KIVA4 simulations.

4. Conclusions.

The adoption of detailed reaction mechanisms when analysing complex combustion systems, such as internal combustion engines, is becoming mandatory due to the need for accurate predictions not only in terms of overall heat release, but also of kinetics-controlled phenomena such as low temperature chemistry and pollutant formation. However, full mechanisms are still too computationally demanding for practical CFD simulations, even with parallel computing systems. Thus, mechanism reduction is still a viable approach, and this is particularly true when dealing with mechanisms involving large hydrocarbons, where the size of the full reaction system is often of the order of thousands reactions and species. However, simple mechanism reduction where the reduced mechanism consists of a limited set of reactions can lead to mechanisms with a limited validity range. The present approach for the reduction and optimization of detailed reaction mechanisms features element-flux analysis to identify and select the number and the corresponding set of species to retain in the reduced mechanism, and a single objective, binary coded genetic algorithm optimizer for the calibration of select reaction rate parameters. This procedure was included into an automatic algorithm which proceeds progressively. The advantage of the iterative procedure is that the optimization is likely to reach the optimum value even with a limited number of merit function evaluations, when compared to the approach of including all possible values of the variables to be optimized.

28

The procedure was applied to the generation of a reduced mechanism for ethanol oxidation, suitable for internal combustion engine simulations. Starting from the full LLNL mechanism, it achieved a reduced mechanism consisting of 33 species and 155 reactions. It is interesting to point out that agreed better with experiments than the detailed LLNL mechanism. The mechanism validity range was kept as broad as possible for use in internal combustion engine simulations. Smaller mechanisms may be developed for more limited validity ranges, but this may lead to faulty predictions at engine-like conditions. In the method the Arrhenius parameters are consistent with the experimental uncertainties reported in literature.

5. Acknowledgements.

Appendix A. Reduced and optimized mechanism for ethanol ignition.

No.	Reaction	A	b	E
1.	$H_2 + OH <=> H + H_2O$	+2.140e+008	1.52	+3.449e+003
2.	$O + OH <=> H + O_2$	+2.020e+014	-0.40	+0.000e+000
3.	$H_2 + O <=> H + OH$	+5.060e+004	2.67	+6.290e+003
4.	$H + O_2(+M) <=> HO_2(+M)$	+4.520e+013	0.00	+0.000e+000
	LOW / +1.05e+019 -1.26 +0.00e+000 /			
	Enhanced third-body efficiencies:			
	H_2/0.00/ CH_4/10.00/ CO_2/3.80/ CO/1.90/ H_2O/0.00/ N_2/0.00/			
5.	$H + O_2(+N_2) <=> HO_2(+N_2)$	+4.520e+013	0.00	+0.000e+000
	LOW / +2.03e+020 -1.59 +0.00e+000 /			
6.	$H + O_2(+H_2) <=> HO_2(+H_2)$	+4.520e+013	0.00	+0.000e+000
	LOW / +1.52e+019 -1.13 +0.00e+000 /			
7.	$H + O_2(+H_2O) <=> HO_2(+H_2O)$	+4.520e+013	0.00	+0.000e+000
	LOW / +2.10e+023 -2.44 +0.00e+000 /			
8.	$OH + HO_2 <=> O_2 + H_2O$	+2.130e+028	-4.83	+3.500e+003
	(Duplicate reaction)			
9.	$OH + HO_2 <=> O_2 + H_2O$	+9.100e+014	0.00	+1.096e+004
	(Duplicate reaction)			
10.	$H + HO_2 <=> 2OH$	+1.500e+014	0.00	+1.000e+003

11.	$H + HO_2 <=> H_2 + O_2$	+6.630e+013	0.00	+2.126e+003
12.	$H + HO_2 <=> O + H_2O$	+3.010e+013	0.00	+1.721e+003
13.	$O + HO_2 <=> O_2 + OH$	+3.250e+013	0.00	+0.000e+000
14.	$2OH <=> O + H_2O$	+3.570e+004	2.40	-2.112e+003
15.	$2H <=> H_2$	+1.000e+018	-1.00	+0.000e+000
16.	$H_2 + 2H <=> 2H_2$	+9.200e+016	-0.60	+0.000e+000
17.	$2H + H_2O <=> H_2 + H_2O$	+6.000e+019	-1.25	+0.000e+000
18.	$H + OH <=> H_2O$	+2.210e+022	-2.00	+0.000e+000
19.	$H + O <=> OH$	+4.710e+018	-1.00	+0.000e+000
20.	$2O <=> O_2$	+1.890e+013	0.00	-1.788e+003
21.	$2HO_2 <=> O_2 + H_2O_2$	+4.200e+014	0.00	+1.198e+004
	(Duplicate reaction)			
22.	$2HO_2 <=> O_2 + H_2O_2$	+1.300e+011	0.00	-1.629e+003
	(Duplicate reaction)			
23.	$2OH(+M) <=> H_2O_2(+M)$	+1.240e+014	-0.37	+0.000e+000
	LOW / +3.04e+030 -4.63 +2.05e+003 /			
	TROE / +4.70e-001 +1.00e+002 +2.00e+003 +1.00e+015 /			
24.	$H + H_2O_2 <=> H_2 + HO_2$	+1.980e+006	2.00	+2.435e+003
25.	$H + H_2O_2 <=> OH + H_2O$	+3.070e+013	0.00	+4.217e+003
26.	$O + H_2O_2 <=> OH + HO_2$	+9.550e+006	2.00	+3.970e+003
27.	$OH + H_2O_2 <=> HO_2 + H_2O$	+2.400e+000	4.04	-2.162e+003
28.	$H + CH_3(+M) <=> CH_4(+M)$	+2.140e+015	-0.40	+4.286e+000
	LOW / +3.31e+030 -4.00 +2.11e+003 /			
	TROE / +0.00e+000 +1.00e-015 +1.00e-015 +4.00e+001 /			
	Enhanced third-body efficiencies:			
	$H_2/2.00/ CO_2/3.00/ CO/2.00/ H_2O/5.00/$			
29.	$H + CH_4 <=> H_2 + CH_3$	+6.914e+003	3.00	+9.875e+003
30.	$CH_4 + OH <=> CH_3 + H_2O$	+5.148e+006	2.00	+2.547e+003
31.	$CH_4 + O <=> CH_3 + OH$	+8.502e+008	1.56	+9.940e+003
32.	$CH_4 + HO_2 <=> CH_3 + H_2O_2$	+1.120e+013	0.00	+2.886e+004
33.	$CH_3 + HO_2 <=> CH_4 + O_2$	+9.429e+011	0.00	+4.286e+000
34.	$CH_3 + O <=> H + CH_2O$	+1.531e+014	0.00	+0.000e+000
35.	$CH_3 + O_2 <=> CH_2O + OH$	+4.805e+011	0.00	+1.276e+004
36.	$H + CH_2OH <=> CH_3 + OH$	+1.914e+013	0.00	+1.429e+000
37.	$CH_3 + OH <=> H_2O + CH_2(S)$	+2.000e+013	0.00	+5.736e+002
38.	$CH_3 + OH <=> CH_2 + H_2O$	+5.057e+006	2.00	+2.500e+003
39.	$H + CH_3 <=> H_2 + CH_2$	+4.886e+013	0.00	+1.575e+004
40.	$CH_3 <=> H + CH_2$	+2.334e+016	0.00	+9.925e+004
41.	$H + CH_2O(+M) <=> CH_2OH(+M)$	+6.634e+011	0.45	+3.600e+003
	LOW / +9.10e+031 -4.82 +6.53e+003 /			

TROE / +7.19e-001 +1.03e+002 +1.29e+003 +4.16e+003 /

Enhanced third-body efficiencies:

$H_2O/5.00/$

42.	$H + CH_2OH <=> H_2 + CH_2O$	+3.829e+013	0.00	+1.429e+000
43.	$OH + CH_2OH <=> CH_2O + H_2O$	+1.000e+013	0.00	+7.143e+000
44.	$O + CH_2OH <=> CH_2O + OH$	+3.143e+012	0.00	+4.286e+000
45.	$O_2 + CH_2OH <=> CH_2O + HO_2$	+4.934e+014	-1.00	+2.857e+000
	(Duplicate reaction)			
46.	$O_2 + CH_2OH <=> CH_2O + HO_2$	+5.577e+013	0.00	+3.117e+003
	(Duplicate reaction)			
47.	$CH_2 + OH <=> H + CH_2O$	+4.786e+013	0.00	+1.429e+000
48.	$CH_2 + CO_2 <=> CH_2O + CO$	+3.457e+010	0.00	+1.000e+003
49.	$CH_2 + O <=> 2H + CO$	+1.571e+013	0.00	+1.429e+000
50.	$CH_2 + O <=> H_2 + CO$	+3.000e+013	0.00	+7.143e+000
51.	$CH_2 + O_2 <=> CH_2O + O$	+6.298e+021	-3.30	+2.745e+003
52.	$CH_2 + O_2 <=> 2H + CO_2$	+2.538e+021	-3.30	+2.745e+003
53.	$CH_2 + O_2 <=> H_2 + CO_2$	+5.483e+020	-3.30	+1.637e+003
54.	$CH_2 + O_2 <=> CO + H_2O$	+7.280e+019	-2.54	+1.576e+003
55.	$CH_2 + O_2 <=> HCO + OH$	+1.880e+020	-3.30	+3.327e+002
56.	$CH_3 + CH_2 <=> H + C_2H_4$	+3.086e+013	0.00	+2.857e+000
57.	$2CH_2 <=> 2H + C_2H_2$	+1.257e+013	0.00	+0.000e+000
58.	$CH_2(S) <=> CH_2$	+3.143e+012	0.00	+5.714e+000
59.	$CH_4 + CH_2(S) <=> 2CH_3$	+3.086e+013	0.00	+1.000e+001
60.	$O_2 + CH_2(S) <=> H + CO + OH$	+5.400e+013	0.00	+5.714e+000
61.	$H_2 + CH_2(S) <=> H + CH_3$	+7.000e+013	0.00	+0.000e+000
62.	$O + CH_2(S) <=> 2H + CO$	+1.629e+013	0.00	+1.000e+001
63.	$OH + CH_2(S) <=> H + CH_2O$	+3.686e+013	0.00	+1.000e+001
64.	$CO_2 + CH_2(S) <=> CH_2O + CO$	+5.057e+012	0.00	+4.286e+000
65.	$CH_3 + CH_2(S) <=> H + C_2H_4$	+1.086e+013	0.00	+1.000e+001
66.	$HCOOH <=> CO + H_2O$	+3.045e+014	0.00	+4.733e+004
67.	$HCOOH <=> H_2 + CO_2$	+1.041e+015	0.00	+6.060e+004
68.	$OH + HCOOH <=> H + CO_2 + H_2O$	+3.818e+006	2.06	+8.375e+002
69.	$OH + HCOOH <=> CO + OH + H_2O$	+2.273e+007	1.50	-9.620e+002
70.	$H + HCOOH <=> H_2 + H + CO_2$	+3.271e+006	2.10	+5.703e+003
71.	$H + HCOOH <=> H_2 + CO + OH$	+6.060e+013	-0.35	+2.860e+003
72.	$CH_3 + HCOOH <=> CH_4 + CO + OH$	+3.900e-007	5.80	+2.577e+003
73.	$HO_2 + HCOOH <=> CO + OH + H_2O_2$	+3.497e+019	-2.20	+1.223e+004
74.	$O + HCOOH <=> CO + 2OH$	+5.563e+017	-1.90	+3.357e+003
75.	$CH_2O + OH <=> HCO + H_2O$	+3.430e+009	1.18	-5.236e+002
76.	$H + CH_2O <=> H_2 + HCO$	+6.883e+007	1.77	+3.514e+003

77.	$CH_2O <=> H + HCO$	+1.797e+016	0.00	+8.447e+004
78.	$CH_2O + O <=> HCO + OH$	+5.657e+012	0.00	+3.212e+003
79.	$HCO + O_2 <=> CO + HO_2$	+1.105e+013	0.00	+4.100e+002
80.	$HCO <=> H + CO$	+2.710e+017	-1.00	+1.481e+004
81.	$HCO + OH <=> CO + H_2O$	+1.000e+014	0.00	+2.857e+000
82.	$H + HCO <=> H_2 + CO$	+1.462e+013	0.25	+5.714e+000
83.	$HCO + O <=> CO + OH$	+3.686e+013	0.00	+1.429e+000
84.	$HCO + O <=> H + CO_2$	+3.000e+013	0.00	+2.857e+000
85.	$CO + OH <=> H + CO_2$	+9.420e+003	2.25	-2.351e+003
86.	$CO + O <=> CO_2$	+6.170e+014	0.00	+3.000e+003
87.	$CO + O_2 <=> CO_2 + O$	+2.530e+012	0.00	+4.769e+004
88.	$CO + HO_2 <=> CO_2 + OH$	+5.800e+013	0.00	+2.293e+004
89.	$C_2H_5OH(+M) <=> CH_3 + CH_2OH(+M)$	+7.298e+023	-1.68	+8.335e+004
	LOW / +2.88e+085 -18.90 +1.10e+005 /			
	TROE / +5.00e-001 +2.00e+002 +8.90e+002 +4.60e+003 /			
	Enhanced third-body efficiencies:			
	H_2/2.00/ CO_2/3.00/ CO/2.00/ H_2O/5.00/			
90.	$C_2H_5OH(+M) <=> OH + C_2H_5(+M)$	+1.536e+023	-1.54	+9.601e+004
	LOW / +3.25e+085 -18.81 +1.15e+005 /			
	TROE / +5.00e-001 +3.00e+002 +9.00e+002 +5.00e+003 /			
	Enhanced third-body efficiencies:			
	H_2/2.00/ CO_2/3.00/ CO/2.00/ H_2O/5.00/			
91.	$C_2H_5OH(+M) <=> H_2O + C_2H_4(+M)$	+5.341e+013	0.09	+7.747e+004
	LOW / +2.57e+083 -18.85 +8.65e+004 /			
	TROE / +7.00e-001 +3.50e+002 +8.00e+002 +3.80e+003 /			
	Enhanced third-body efficiencies:			
	H_2O/5.00/			
92.	$C_2H_5OH(+M) <=> H_2 + CH_3HCO(+M)$	+3.930e+011	0.10	+9.881e+004
	LOW / +4.46e+087 -19.42 +1.16e+005 /			
	TROE / +9.00e-001 +9.00e+002 +1.10e+003 +3.50e+003 /			
	Enhanced third-body efficiencies:			
	H_2O/5.00/			
93.	$OH + C_2H_5OH <=> H_2O + C_2H_4OH$	+1.740e+011	0.27	+6.514e+002
94.	$OH + C_2H_5OH <=> H_2O + CH_3CHOH$	+6.761e+011	0.15	+2.857e+000
95.	$OH + C_2H_5OH <=> H_2O + CH_3CH_2O$	+2.345e+011	0.30	+1.704e+003
96.	$H + C_2H_5OH <=> H_2 + C_2H_4OH$	+2.355e+007	1.80	+4.880e+003
97.	$H + C_2H_5OH <=> H_2 + CH_3CHOH$	+4.939e+007	1.65	+2.585e+003
98.	$H + C_2H_5OH <=> H_2 + CH_3CH_2O$	+2.186e+007	1.60	+3.298e+003
99.	$O + C_2H_5OH <=> OH + C_2H_4OH$	+1.801e+008	1.70	+5.225e+003
100.	$O + C_2H_5OH <=> OH + CH_3CHOH$	+1.450e+007	1.85	+1.980e+003

101.	$O + C_2H_5OH <=> OH + CH_3CH_2O$	+2.302e+007	2.00	+4.448e+003
102.	$CH_3 + C_2H_5OH <=> CH_4 + C_2H_4OH$	+6.883e+001	3.18	+9.210e+003
103.	$CH_3 + C_2H_5OH <=> CH_4 + CH_3CHOH$	+3.952e+002	2.99	+6.926e+003
104.	$CH_3 + C_2H_5OH <=> CH_4 + CH_3CH_2O$	+1.119e+002	2.99	+8.960e+003
105.	$HO_2 + C_2H_5OH <=> H_2O_2 + CH_3CHOH$	+8.200e+003	2.55	+1.075e+004
106.	$HO_2 + C_2H_5OH <=> H_2O_2 + C_2H_4OH$	+1.230e+004	2.55	+1.373e+004
107.	$HO_2 + C_2H_5OH <=> H_2O_2 + CH_3CH_2O$	+3.643e+012	0.00	+2.811e+004
108.	$CH_3CH_2O <=> H + CH_3HCO$	+8.949e+034	-5.89	+2.419e+004
109.	$CH_3CH_2O <=> CH_3 + CH_2O$	+2.276e+038	-6.96	+2.686e+004
110.	$O_2 + CH_3CH_2O <=> HO_2 + CH_3HCO$	+2.171e+010	0.00	+1.053e+003
111.	$CO + CH_3CH_2O <=> CO_2 + C_2H_5$	+8.959e+002	3.16	+6.072e+003
112.	$H + CH_3CH_2O <=> CH_3 + CH_2OH$	+3.000e+013	0.00	+8.571e+000
113.	$H + CH_3CH_2O <=> H_2O + C_2H_4$	+9.429e+012	0.00	+8.571e+000
114.	$OH + CH_3CH_2O <=> H_2O + CH_3HCO$	+1.914e+013	0.00	+2.857e+000
115.	$O_2 + CH_3CHOH <=> HO_2 + CH_3HCO$	+1.515e+014	0.00	+4.802e+003
	(Duplicate reaction)			
116.	$O_2 + CH_3CHOH <=> HO_2 + CH_3HCO$	+2.649e+015	-1.20	+2.857e+000
	(Duplicate reaction)			
117.	$O + CH_3CHOH <=> OH + CH_3HCO$	+1.686e+014	0.00	+0.000e+000
118.	$H + CH_3CHOH <=> H_2O + C_2H_4$	+5.743e+013	0.00	+4.286e+000
119.	$H + CH_3CHOH <=> CH_3 + CH_2OH$	+4.371e+013	0.00	+1.429e+000
120.	$HO_2 + CH_3CHOH <=> 2OH + CH_3HCO$	+6.743e+013	0.00	+8.571e+000
121.	$OH + CH_3CHOH <=> H_2O + CH_3HCO$	+9.571e+012	0.00	+0.000e+000
122.	$CH_3CHOH <=> H + CH_3HCO$	+3.143e+013	0.00	+2.393e+004
123.	$OH + CH_3HCO <=> CH_3 + HCOOH$	+5.743e+015	-1.08	+1.429e+000
124.	$H + C_2H_5 <=> H_2 + C_2H_4$	+6.786e+013	0.00	+7.657e+003
125.	$H + C_2H_5 <=> 2CH_3$	+3.000e+013	0.00	+8.571e+000
126.	$OH + C_2H_5 <=> H_2O + C_2H_4$	+7.657e+013	0.00	+5.714e+000
127.	$O + C_2H_5 <=> CH_3 + CH_2O$	+1.229e+014	0.00	+7.143e+000
128.	$HO_2 + C_2H_5 <=> OH + CH_3CH_2O$	+2.314e+013	0.00	+1.000e+001
129.	$O_2 + C_2H_5 <=> HO_2 + C_2H_4$	+4.211e+028	-5.40	+7.910e+003
130.	$O_2 + C_2H_5 <=> OH + CH_3HCO$	+7.140e+011	-0.48	+9.073e+003
131.	$OH + C_2H_4 <=> C_2H_4OH$	+1.290e+012	0.00	-7.820e+002
132.	$O_2 + C_2H_4OH <=> HOC_2H_4O_2$	+1.457e+012	0.00	-1.100e+003
133.	$HOC_2H_4O_2 <=> 2CH_2O + OH$	+7.371e+010	0.00	+2.765e+004
134.	$OH + C_2H_4 <=> H_2O + C_2H_3$	+2.020e+013	0.00	+6.699e+003
135.	$O + C_2H_4 <=> CH_3 + HCO$	+1.253e+007	1.88	+1.867e+002
136.	$CH_3 + C_2H_4 <=> CH_4 + C_2H_3$	+3.594e+000	3.70	+1.113e+004
137.	$H + C_2H_4 <=> H_2 + C_2H_3$	+1.056e-007	6.00	+1.982e+003
138.	$H + C_2H_4(+M) <=> C_2H_5(+M)$	+3.394e+011	0.45	+2.134e+003

LOW / +1.11e+034 -5.00 +4.45e+003 /

TROE / +1.00e+000 +1.00e-015 +9.50e+001 +2.00e+002 /

Enhanced third-body efficiencies:

$H_2/2.00/ CO_2/3.00/ CO/2.00/ H_2O/5.00/$

139.	$C_2H_4(+M) <=> H_2 + C_2H_2(+M)$	+3.446e+014	0.00	+7.954e+004

LOW / +1.50e+015 0.00 +5.54e+004 /

140.	$H + C_2H_3(+M) <=> C_2H_4(+M)$	+1.168e+013	0.27	+2.920e+002

LOW / +9.80e+029 -3.86 +3.32e+003 /

TROE / +7.82e-001 +2.08e+002 +2.66e+003 +6.10e+003 /

Enhanced third-body efficiencies:

$H_2O/5.00/$

141.	$H + C_2H_3 <=> H_2 + C_2H_2$	+1.723e+014	0.00	+5.714e+000
142.	$O_2 + C_2H_3 <=> CH_2O + HCO$	+5.343e+028	-5.31	+7.614e+003
143.	$O_2 + C_2H_3 <=> HO_2 + C_2H_2$	+1.151e-006	6.00	+8.265e+003
144.	$OH + C_2H_3 <=> H_2O + C_2H_2$	+1.086e+013	0.00	+5.714e+000
145.	$C_2H + C_2H_3 <=> 2C_2H_2$	+5.057e+013	0.00	+1.000e+001
146.	$CH_3 + C_2H_3 <=> CH_4 + C_2H_2$	+3.371e+013	0.00	+1.429e+000
147.	$OH + C_2H_2 <=> H_2O + C_2H$	+5.681e+007	2.00	+1.340e+004
148.	$OH + C_2H_2 <=> CH_3 + CO$	+9.246e-004	4.00	-2.086e+003
149.	$O + C_2H_2 <=> CH_2 + CO$	+1.923e+006	2.00	+1.656e+003
150.	$O + C_2H_2 <=> OH + C_2H$	+1.715e+015	-0.60	+1.307e+004
151.	$CH_3 + C_2H_2 <=> CH_4 + C_2H$	+5.689e+010	0.00	+1.655e+004
152.	$C_2H_2 <=> H + C_2H$	+5.160e+016	0.00	+1.070e+005
153.	$H + C_2H_2(+M) <=> C_2H_3(+M)$	+5.243e+011	0.58	+2.367e+003

LOW / +2.25e+040 -7.27 +6.58e+003 /

TROE / +1.00e+000 +1.00e-015 +6.75e+002 +1.00e+015 /

Enhanced third-body efficiencies:

$H_2/2.00/ CO_2/3.00/ CO/2.00/ H_2O/5.00/$

154.	$H_2 + C_2H <=> H + C_2H_2$	+6.895e+005	2.39	+1.012e+003
155.	$O_2 + C_2H <=> H + 2CO$	+1.731e+013	0.00	-4.766e+002

Table A.3: 155 reactions and 33 species reduced and optimized reaction mechanism for ethanol ignition. Rate constants $k = AT^b exp(-E/R_uT)$; units are cm, mol, s, cal, K.

References

[1] T. Lu, C. K. Law, Progress in Energy and Combustion Science 35 (2009) 192 – 215.

[2] C. K. Law, Proceedings of the Combustion Institute 31 (2007) 1 – 29.

[3] J. M. Simmie, Progress in Energy and Combustion Science 29 (2003) 599 – 634.

[4] J. Warnatz, Proceedings of the Combustion Institute 18 (1981) 369–384.

[5] C. K. Westbrook, J. Warnatz, W. J. Pitz, Proceedings of the Combustion Institute 22 (1989) 893 – 901.

[6] R. P. Lindstedt, L. Q. Maurice, Combustion Science and Technology 107 (1995) 317 – 353.

[7] H. Curran, P. Gaffuri, W. Pitz, C. Westbrook, Combustion and Flame 114 (1998) 149 – 177.

[8] N. M. Marinov, International Journal of Chemical Kinetics 31 (1999) 183 – 220.

[9] S. L. Fischer, F. L. Dryer, H. J. Curran, International Journal of Chemical Kinetics 32 (2000) 713 – 740.

[10] H. J. Curran, P. Gaffuri, W. J. Pitz, C. K. Westbrook, Combustion and Flame 129 (2002) 253 – 280.

[11] O. Herbinet, W. J. Pitz, C. K. Westbrook, Combustion and Flame 157 (2010) 893 – 908.

[12] S.-C. Kong, R. D. Reitz, Proceedings of the Combustion Institute 29 (2002) 663 – 669.

[13] R. M. Hanson, S. L. Kokjohn, D. A. Splitter, R. D. Reitz, SAE International Journal of Engines 3 (2010) 700–716.

[14] K. He, M. G. Ierapetritou, I. P. Androulakis, Combustion and Flame 155 (2008) 585 – 604.

[15] K. Edwards, T. F. Edgar, V. I. Manousiouthakis, Computers & Chemical Engineering 22 (1998) 239 – 246.

[16] I. P. Androulakis, J. M. Grenda, J. W. Bozzelli, AIChE Journal 50 (2004) 2956 – 2970.

[17] L. Elliott, D. B. Ingham, A. G. Kyne, N. S. Mera, M. Pourkashanian, C. W. Wilson, Journal of Engineering for Gas Turbines and Power 128 (2006) 255–263.

[18] I. Banerjee, M. G. Ierapetritou, Combustion and Flame 144 (2006) 619 – 633.

[19] M. Janbozorgi, S. Ugarte, H. Metghalchi, J. C. Keck, Combustion and Flame 156 (2009) 1871 – 1885.

[20] L. Liang, J. G. Stevens, J. T. Farrell, Proceedings of the Combustion Institute 32 (2009) 527 – 534.

[21] K. He, I. P. Androulakis, M. G. Ierapetritou, Chemical Engineering Science 65 (2010) 1173 – 1184.

[22] K. He, M. G. Ierapetritou, I. P. Androulakis, AIChE Journal 56 (2010) 1305 – 1314.

[23] Y. Shi, H.-W. Ge, J. L. Brakora, R. D. Reitz, Energy & Fuels 24 (2010) 1646–1654.

[24] H. Rabitz, M. Kramer, D. Dacol, Annual Review of Physical Chemistry 34 (1983) 419–461.

[25] T. Turanyi, New Journal of Chemistry 14 (1990) 795 – 803.

[26] T. Lu, C. K. Law, Proceedings of the Combustion Institute 30 (2005) 1333 – 1341.

[27] P. Pepiot-Desjardins, H. Pitsch, Combustion and Flame 154 (2008) 67 – 81.

[28] N. J. Brown, G. Li, M. L. Koszykowski, International Journal of Chemical Kinetics 29 (1997) 393 – 414.

[29] P. Gokulakrishnan, A. Lawrence, P. McLellan, E. Grandmaison, Computers & Chemical Engineering 30 (2006) 1093 – 1101.

[30] J. Revel, J. C. Boettner, M. Cathonnet, J. S. Bachman, Journal de chimie physique 91 (1994) 365 – 382.

[31] B. Bhattacharjee, D. A. Schwer, P. I. Barton, W. H. Green, Combustion and Flame 135 (2003) 191 – 208.

[32] L. Elliott, D. B. Ingham, A. G. Kyne, N. S. Mera, M. Pourkashanian, C. W. Wilson, Progress in Energy and Combustion Science 30 (2004) 297 – 328.

[33] L. Elliott, D. B. Ingham, A. G. Kyne, N. S. Mera, M. Pourkashanian, C. W. Wilson, Industrial & Engineering Chemistry Research 44 (2005) 658–667.

[34] L. Elliott, D. B. Ingham, A. G. Kyne, N. S. Mera, M. Pourkashanian, S. Whittaker, Computers & Chemical Engineering 30 (2006) 889 – 900.

[35] O. O. Oluwole, B. Bhattacharjee, J. E. Tolsma, P. I. Barton, W. H. Green, Combustion and Flame 146 (2006) 348 – 365.

[36] O. O. Oluwole, P. I. Barton, W. H. Green, Combustion Theory and Modelling 11 (2007) 127–146.

[37] M. Bodenstein, Z. Phys. Chem 85 (1913) 329 – 397.

[38] L. Underhill, D. Chapman, J. Chem. Soc. Trans. 103 (1913) 496 – 508.

[39] M. R. Roussel, S. J. Fraser, The Journal of Chemical Physics 93 (1990) 1072–1081.

[40] S. Lam, D. Goussis, Proceedings of the Combustion Institute 22 (1989) 931 – 941.

[41] S. H. Lam, D. A. Goussis, International Journal of Chemical Kinetics 26 (1994) 461–486.

[42] T. Lu, Y. Ju, C. K. Law, Combustion and Flame 126 (2001) 1445 – 1455.

[43] M. Valorani, F. Creta, D. A. Goussis, J. C. Lee, H. N. Najm, Combustion and Flame 146 (2006) 29 – 51.

[44] A. Massias, D. Diamantis, E. Mastorakos, D. Goussis, Combustion and Flame 117 (1999) 685 – 708.

[45] J. Prager, H. N. Najm, M. Valorani, D. A. Goussis, Proceedings of the Combustion Institute 32 (2009) 509 – 517.

[46] U. Maas, S. Pope, Combustion and Flame 88 (1992) 239 – 264.

[47] S. Pope, U. Maas, Simplifying chemical kinetics: trajectory-generated low-dimensional manifolds, Technical Report, Cornell University, 1993.

[48] C. Gear, I. Kevrekidis, Journal of Scientific Computing 25 (2005) 17–28. 10.1007/BF02728980.

[49] J. C. Keck, D. Gillespie, Combustion and Flame 17 (1971) 237 – 241.

[50] J. C. Keck, Progress in Energy and Combustion Science 16 (1990) 125 – 154.

[51] A. N. Gorban, I. V. Karlin, Chemical Engineering Science 58 (2003) 4751 – 4768. International Symposium on Mathematics in Chemical Kinetics and Engineering.

[52] Z. Ren, S. B. Pope, A. Vladimirsky, J. M. Guckenheimer, The Journal of Chemical Physics 124 (2006) 114111.

[53] D. Lebiedz, V. Reinhardt, J. Siehr, Journal of Computational Physics 229 (2010) 6512 – 6533.

[54] C. T. Bowman, R. K. Hanson, W. C. Gardiner, V. Lissianski, M. Frenklach, M. Goldenberg, G. P. Smith, D. R. Crosley, D. M. Golden, GRI-Mech 2.11–An Optimized Detailed Chemical Reaction Mechanism for Methane Combustion and NO Formation and Reburning., Technical Report, GRI Topical Report 97/0020., 1997.

[55] M. Frenklach, H. Wang, M. Goldenberg, , G. P. Smith, D. M. Golden, C. T. Bowman, R. K. Hanson, W. C. Gardiner, V. Lissianski, GRI-Mech–An Optimized Detailed Chemical Reaction Mechanism for Methane Combustion., Technical Report, GRI Topical Record 95/0058, 1995.

[56] L. Elliott, D. Ingham, A. Kyne, N. Mera, M. Pourkashanian, C. Wilson, Combustion Science and Technology 175 (2003) 619 – 648.

[57] W. Jones, R. Lindstedt, Combustion and Flame 73 (1988) 233 – 249.

[58] E. Fernández-Tarrazo, A. L. Sánchez, A. Linán, F. A. Williams, Combustion and Flame 147 (2006) 32 – 38.

[59] B. Franzelli, E. Riber, M. Sanjosé, T. Poinsot, Combustion and Flame 157 (2010) 1364 – 1373.

[60] W. Mallard, F. Westley, J. Herron, R. Hampson, D. Frizzell, Nist chemical kinetics database on the web, 2000. Standard Reference Database 17, Version 7.0 (Web Version), Release 1.5.

[61] V. Kondratiev, V. Azatyan, Proceedings of the Combustion Institute 14 (1973) 37 – 44.

[62] R. Walker, Proceedings of the Combustion Institute 22 (1989) 883 – 892.

[63] M. Mitchell, An Introduction to Genetic Algorithms, MIT Press, Cambridge, MA, 1996.

[64] I. P. Androulakis, AIChE Journal 46 (2000) 361 – 371.

[65] C. J. Montgomery, C. Yang, A. R. Parkinson, J.-Y. Chen, Combustion and Flame 144 (2006) 37 – 52.

[66] J. J. Hernández, R. Ballesteros, J. Sanz-Argent, Mathematical and Computer Modelling 52 (2010) 1185 – 1193. Mathematical Models in Medicine, Business & Engineering 2009.

[67] V. Hamosfakidis, R. D. Reitz, Combustion and Flame 132 (2003) 433 – 450.

[68] J. Warnatz, U. Maas, R. W. Dibble, Combustion: Physical and Chemical Fundamentals, Modeling and Simulation, Experiments, Pollutant Formation, Springer, 2006.

[69] R. J. Kee, F. M. Rupley, E. Meeks, J. A. Miller, CHEMKIN-III: a FORTRAN chemical kinetics package for the analysis of gasphase chemical and plasma kinetics, Technical Report, Sandia National Laboratories, 1996. SAND96-8216.

[70] R. G. Gilbert, K. Luther, J. Troe, Berichte der Bunsengesellschaft fur physikalische Chemie 87 (1983) 169–177.

[71] P. Stewart, C. Larson, D. Golden, Combustion and Flame 75 (1989) 25 – 31.

[72] E. Mattarelli, F. Perini, C. A. Rinaldini, SAE International Journal of Engines 2 (2009) 199–210.

[73] H. J. Curran, M. P. Dunphy, J. M. Simmie, C. K. Westbrook, W. J. Pitz, Proceedings of the Combustion Institute 24 (1992) 769 – 776. Twenty-Fourth Symposium on Combustion.

[74] M. Sjöberg, J. E. Dec, SAE International Journal of Engines 2 (2009) 492–510.

[75] D. J. Torres, M. F. Trujillo, Journal of Computational Physics 219 (2006) 943 – 975.